Mechanistic Modeling of Nitrite Accumulation and Nitrogen Oxide Gas Emissions during Nitrification

R. T. Venterea* and D. E. Rolston

ABSTRACT

Nitrite (NO_2^-) accumulation in soil following nitrogen (N) fertilizer application has been observed under a variety of conditions. The presence of NO_2^- together with soil acidity results in the formation of nitrous acid (HNO_2), which decomposes abiotically to produce nitric oxide (NO) and nitrous oxide (N_2O). These N oxide trace gases have potential effects on several atmospheric processes. Presented here is a model that describes some of the interactions between microbial, chemical, and physical processes that influence NO_2^- accumulation and N oxide gas emissions following applications of NH_4^+–based fertilizers. The model is applied to hypothetical and actual field scenarios. A two-step, two-population nitrification submodel is linked to gas production and transformation submodels. Transport of all chemical species occurs by diffusion. The model results suggest that some degree of transient nitrite accumulation following NH_4^+ application is a consequence of the nature of nitrification itself. Model simulations and sensitivity analysis indicate that (i) soils receiving similar fertilizer treatments but differing in their ability to buffer nitrification-induced acidity may produce dramatically different N oxide gas emissions, (ii) subsurface fertilizer placement can significantly reduce net NO emissions, and (iii) the differential responses of *Nitrosomonas* and *Nitrobacter* populations to chemical toxicities associated with the form and/or rate of fertilizer application may significantly affect the extent of NO_2^- accumulation and corresponding gas emissions. Overall, the results contribute to our basic understanding of how multiple microbial, chemical, and physical factors can interact to control the net soil-to-atmosphere emission of nitrification-derived NO and N_2O.

NITRITE accumulation in soil following N fertilizer application has been observed under a variety of conditions (Martin et al., 1942; Chapman and Leibeg, 1952; Morrill and Dawson, 1967; Bezdicek et al., 1971; Paul and Domsch, 1972; Chalk et al., 1975; Burns et al., 1995). The presence of NO_2^- can promote abiotic reactions involving HNO_2, which decomposes chemically to form NO and N_2O gases (Nelson, 1982). Nitrogen losses in the form of NO and N_2O have potential effects on several atmospheric processes (Crutzen, 1981). A conceptual "hole-in-the-pipe" model describing N oxide gas release from soil has been proposed by Firestone and Davidson (1989). Empirical models have also been developed based on fertilizer N inputs and soil temperature (Williams et al., 1992). The need for more mechanistic, process-based models has been identified as important for at least two reasons: (i) to assist in developing management strategies for minimizing gaseous N losses from agricultural systems and (ii) to help reduce uncertainties in regional and global assessments of the importance of soils as sources of N oxide gases (Mosier et al., 1996; Davidson and Kingerlee, 1997; Matson, 1997; Matson et al., 1998).

The phenomenon of NO_2^- accumulation in soil has generally been attributed to the nitrification process (Van Cleemput and Samater, 1996). In order for NO_2^- to accumulate during nitrification, the activity of *Nitrobacter* bacteria, which catalyze the second step of the nitrification sequence (i.e., the oxidation of NO_2^- to nitrate [NO_3^-]), must be less than that of *Nitrosomonas* and other bacteria that catalyze the first step of the sequence (i.e., the oxidation of ammonium [NH_4^+] to NO_2^-). Reduced *Nitrobacter* activity has been attributed to slower growth rates in response to N additions (i.e., lag effects) compared with NH_4^+–oxidizer populations (Morrill and Dawson, 1967) and/or to the sensitivity of *Nitrobacter* populations to toxicity effects associated with free NH_3, nitrification-induced acidity, or other chemical factors (Bezdicek et al., 1971; Venterea and Rolston, 2000a).

Recent studies have quantified kinetic relationships between HNO_2 concentrations and NO and N_2O production rates in several agricultural soils. These studies indicate that even relatively low NO_2^- levels (<1 μg N g^{-1}) can promote significant rates of HNO_2–mediated NO production (Venterea and Rolston, 2000a,b). Because pH and NO_2^- concentrations together determine HNO_2 concentrations and each tend to be highly dynamic during nitrification, a model describing HNO_2–driven NO emissions needs to account for transient nitrification dynamics, accompanying changes in soil pH, and HNO_2–mediated gas production kinetics. In addition, NO is highly reactive and subject to transformation as it diffuses from points of production to the soil–atmosphere interface. Recent studies have also quantified the kinetics of NO-mediated N_2O production under bulk aerobic soil conditions (Venterea and Rolston, 2000b). While detailed models of soil nitrification kinetics and/or biologically mediated N oxide gas emissions have been previously presented, none have described the coupling of these mechanisms (Paul and Domsch, 1972; Ardakani et al., 1974; Darrah et al., 1985; Li et al., 1992; Grant, 1995).

The objective of the present study was to develop a model that describes the microbial and chemical processes influencing HNO_2–driven N oxide gas emissions while accounting for chemical diffusion. The model is applied to hypothetical and actual field scenarios to examine the sensitivity of predicted NO_2^- levels and gas emissions to key parameters and assumptions. The model provides a tool for studying complex interactions between microbial, chemical, and physical factors, while helping to identify areas requiring further investigation.

R.T. Venterea, Institute of Ecosystem Studies, Box AB, Millbrook, NY 12545. D.E. Rolston, Dep. of Land, Air and Water Resources, Univ. of California, One Shields Ave., Davis, CA 95616. Contribution from Dep. of Land, Air and Water Resources, Univ. of California, Davis, CA 95616. Received 31 Jan. 2000. *Corresponding author (venterear@ecostudies.org).

Published in J. Environ. Qual. 29:1741–1751 (2000).

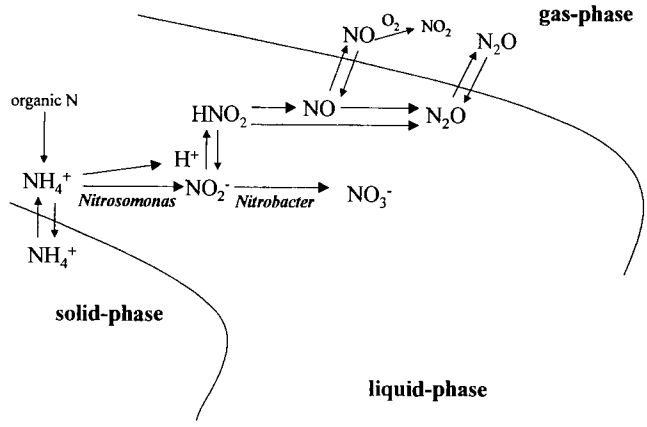

Fig. 1. Transformation mechanisms considered by model. Single (one-way) arrows denote kinetically controlled processes and paired (two-way) arrows denote instantaneous equilibria.

MODEL DESCRIPTION

Scope and Simplifying Assumptions

The dynamics of six chemical components (NH_4^+, NO_2^-, NO_3^-, H^+, NO, and N_2O) and two autotrophic bacterial populations (NH_4^+ oxidizers and NO_2^- oxidizers) under hydrostatic and isothermal conditions are described (Fig. 1). For simplicity, the two classes of bacteria are referred to as *Nitrosomonas* and *Nitrobacter*, respectively, and diversities with respect to growth and activity rates within each population are not considered. The model is applied to conditions of moderate water content ($\leq$0.20 $m^3\ m^{-3}$) and it is assumed that levels of oxygen or carbon dioxide do not limit nitrification rates. Nitrite accumulation and/or N oxide gas production associated with dissimilatory NO_3^- reduction to NO_3^- or NH_4^+ are not considered, although these processes may be important under certain conditions (Firestone and Davidson, 1989; Kelso et al., 1999). While culture studies have indicated that nitrifying organisms can produce NO and N_2O through direct biological means (Conrad, 1995a), the present model considers the primary source of NO production to be the result of abiotic decomposition of biologically generated NO_2^- and HNO_2, based on results of recent experiments with agricultural soils (Venterea and Rolston, 2000a). The subsequent microbial reduction of nitrification-derived NO to N_2O, which has been shown to be important under bulk aerobic soil conditions, is considered (Venterea and Rolston, 2000b). Transport of all chemical species is assumed to be governed by one-dimensional, vertical Fickian diffusion.

Process Description

Processes considered by the model are illustrated in Fig. 1. Ammonium N added as fertilizer or released from soil organic matter (SOM) is subject to nitrification and cation exchange onto soil surfaces. The first step of nitrification, mediated by *Nitrosomonas*, generates NO_2^- and H^+ in molar ratios of 1:1 and 2:1, respectively, in proportion to NH_4^+ oxidized. While the primary biochemical substrate for autotrophic NH_4^+ oxidizers appears to be ammonia (NH_3) and not NH_4^+ (Suzuki et al., 1974), the overall reaction is commonly written with respect to NH_4^+ (e.g., Conrad, 1995b) and kinetic dependencies are often expressed as a function of NH_4^+ concentrations (Paul and Domsch, 1972; Ardakani et al., 1974; Darrah et al., 1985). During nitrification, soil pH responds to the production of H^+ and to buffering reactions that neutralize some of the H^+ that is produced (Wang et al., 1998; Nye, 1972). *Nitrosomonas* populations increase as substrate is utilized (Morrill and Dawson, 1967; Ardakani et al., 1974). The NO_2^- produced is oxidized to NO_3^- by *Nitrobacter* populations, which also proliferate as substrate is utilized (Morrill and Dawson, 1967; Ardakani et al., 1974). The NO_2^- is subject to protonation and formation of HNO_2 (pK_a = 3.3) (Van Cleemput and Samater, 1996):

$$H^+ + NO_2^- \rightleftharpoons HNO_2 \quad [1]$$

Production of NO results in part from aqueous disproportionation of HNO_2–N:

$$3\ HNO_2 \Rightarrow 2\ NO + HNO_3 + H_2O \quad [2]$$

or similar reactions (Van Cleemput et al., 1976). Reactions of HNO_2 with soil organic matter also may result in NO and/or N_2O production (Stevenson, 1994). Additional N_2O production results from microbial NO reduction, which increases with increasing water content (Venterea and Rolston, 2000b). The NO produced is subject to heterotrophic and autotrophic microbial oxidation in the liquid phase and chemical oxidation by O_2 in the gas phase (Fig. 1) (Conrad, 1995b).

Mathematical Description

Chemical Transport and Transformation

Each chemical component is governed by a diffusion–reaction equation, so that the system can be represented as:

$$R_i \frac{\partial C_{j,i}}{\partial t} = \frac{\partial}{\partial z}\left(D_i \frac{\partial C_{j,i}}{\partial z}\right) + P_i \quad [3]$$

where i is the component index, with the correspondence: NH_4^+, i = 1; NO_2^-, i = 2; NO_3^-, i = 3; H^+, i = 4; NO, i = 5; and N_2O, i = 6; $C_{j,i}$ is the concentration (g N m^{-3} or g H^+ m^{-3}) of component i with respect to the component's predominant phase j (i.e., j refers to the gas or liquid phase of soil); R is a phase partitioning parameter ($m^3\ m^{-3}$ soil); P is the net production rate (g m^{-3} soil h^{-1}); t is time (h); z is soil depth (m), and D is the soil diffusivity ($m^3\ m^{-1}$ soil h^{-1}), which is described by Moldrup et al.'s (1997) model:

$$D_i = 0.66\ D_{o,i}\ \kappa\left(\frac{\kappa}{\phi}\right)^{\frac{12-m}{3}} \quad [4]$$

where $D_{o,i}$ is the diffusion coefficient ($m^2\ h^{-1}$) in free liquid or gas of component i, ϕ is total porosity ($m^3\ m^{-3}$ soil), and m = 1 for liquid-phase diffusion and m = 3 for gas-phase diffusion. The parameter κ refers to the volumetric content of the relevant phase, that is, κ is the water content (θ, m^3 H_2O m^{-3} soil) or the gas content (ε, m^3 gas m^{-3} soil) for liquid- and gas-phase diffusion, respectively.

For NH_4^+ (i = 1), a reversible, instantaneous linear relation between solution and sorbed phase is assumed (Wagenet et al., 1977):

$$R_1 = \theta + \rho\ K_{d,1} \quad [5]$$

where ρ is the soil dry bulk density (kg m^{-3}) and $K_{d,1}$ (m^3 H_2O kg^{-1} soil) is the equilibrium liquid–solid partitioning coefficient for NH_4^+. Analogously for NO and N_2O ($i \geq 5$), phase partitioning between gas and liquid phases is described by:

$$R_i = \varepsilon + \frac{\theta}{K_{H,i}} \quad [6]$$

where $K_{H,i}$ is the Henry's law constant (m^3 H_2O m^{-3} gas) for component i. After Wang et al. (1998) and Nye (1972), for H^+ (i = 4), a solid-phase soil pH buffering capacity term

Table 1. Parameters held constant for all model simulations.†

Symbol	Parameter	Value	Units	Reference‡
$D_{o,1}$	aqueous diffusivity, NH_4^+	7.0×10^{-6}	$m^2\ H_2O\ h^{-1}$	1
$D_{o,2}$	aqueous diffusivity, NO_2^-	6.9×10^{-6}	$m^2\ H_2O\ h^{-1}$	1
$D_{o,3}$	aqueous diffusivity, NO_3^-	6.8×10^{-6}	$m^2\ H_2O\ h^{-1}$	1
$D_{o,4}$	aqueous diffusivity, H^+	3.3×10^{-5}	$m^2\ H_2O\ h^{-1}$	2
$D_{o,5}$	gaseous diffusivity, NO	8.5×10^{-2}	m^2 gas h^{-1}	3
$D_{o,6}$	gaseous diffusivity, N_2O	5.2×10^{-2}	m^2 gas h^{-1}	3
$K_{H,5}$	Henry's Law constant, NO	21.2	$m^{-3}\ H_2O\ m^{-3}$ gas	4
$K_{H,6}$	Henry's Law constant, N_2O	1.68	$m^{-3}\ H_2O\ m^{-3}$ gas	4
MR	net NH_4^+ mineralization rate	0.035	mg N kg^{-1} soil h^{-1}	5
$B_{o,1}$	initial *Nitrosomonas* density	2×10^8	cells kg^{-1} soil	6
$K_{s,1}$	half-saturation conc., NH_4^+	2.08	g N m^{-3} H_2O	7
$K_{s,2}$	half-saturation conc., NO_2^-	1.89	g N m^{-3} H_2O	7
$K_{I,1}$	inhibition factor, NH_4^+ oxidation	$10^{-6.3}$	mole H^+ L^{-1}	8,9§
Y_1	yield coef., *Nitrosomonas*	1.7×10^{14}	cells biomass kg^{-1} N	7
Y_2	yield coef., *Nitrobacter*	1.4×10^{14}	cells biomass kg^{-1} N	7
d_1	decay coef., *Nitrosomonas*	0.01	h^{-1}	7#
d_2	decay coef., *Nitrobacter*	0.01	h^{-1}	7#
$k_{red,5}$	rate coef. for NO reduction to N_2O	$32 + 9.2\ S_t$	kg N kg^{-1} NO-N h^{-1}	9††
$k_{G,5}$	rate coef. gas-phase NO oxidation	1.80×10^{-10}	$(kg\ m^{-3})^{-2}\ h^{-1}$	10
L	depth of soil profile	20	cm	¶

† Additional parameters that were varied for Cases 1 through 3 are shown in Table 2.
‡ 1 = Hunik et al., 1994; 2 = Kemper, 1986, 3 = Bird et al., 1960; 4 = Wilhelm et al., 1977; 5 = Curtin et al., 1998; 6 = Morrill and Dawson, 1967; Burns et al., 1995; Bruns et al., 1999; 7 = Keen and Prosser, 1987; 8 = Venterea and Rolston, 2000a; 9 = Venterea and Rolston, 2000b; 10 = Atkinson et al., 1997.
§ $K_{I,1}$ value estimated from published data as described in text.
¶ Value set by authors.
# Calculated from product of maintenance and yield coefficients (Keen and Prosser, 1987).
†† Function of degree of saturation (S_t) calculated from data in Venterea and Rolston (2000b).

accounts for neutralization of acidity produced in liquid phase, so that:

$$R_4 = \theta + \left(\frac{\rho\beta_s}{C_{L,4} \ln 10}\right) \quad [7]$$

where $C_{L,4}$ is the liquid-phase H^+ concentration (g H^+ m^{-3} H_2O) and β_s is the soil buffering capacity (g H^+ kg^{-1} soil pH^{-1}).

The production rate functions (P_i) in Eq. [3] describe the transformation processes for each component (units for some parameters described below are listed in Tables 1 and 2). For NH_4^+ ($i = 1$):

$$P_1 = \rho MR - \left(\frac{\partial C_{L,1}}{\partial t}\right)_{AOR} \quad [8]$$

where MR is the net NH_4^+ mineralization rate. Monod growth and substrate utilization kinetics are used to describe each step of nitrification (Paul and Domsch, 1972; Darrah et al., 1985). The autotrophic NH_4^+ oxidation rate (AOR) in Eq. [8] is therefore given by:

$$\left(\frac{\partial C_{L,1}}{\partial t}\right)_{AOR} = \frac{\rho\ \mu_{max,1}\ C_{L,1}}{K_{s,1} + C_{L,1}}\left(\frac{B_1}{Y_1}\right) \quad [9]$$

where B_1 is the *Nitrosomonas* biomass density, $\mu_{max,1}$ is their maximum specific growth rate, $K_{s,1}$ is the effective half-saturation concentration for growth, and Y_1 is the *Nitrosomonas* yield coefficient. The net production of soil NO_2^- ($i = 2$) is given by:

$$P_2 = \left(\frac{\partial C_{L,1}}{\partial t}\right)_{AOR} - \left(\frac{\partial C_{L,2}}{\partial t}\right)_{NOR} - \theta[HNO_2]_L(k_{PNO} + k_{PN_2O}) \quad [10]$$

where the gross NO_2^- autotrophic oxidation rate (NOR) is defined analogously to Eq. [9], except in this case for NO_2^- utilization by *Nitrobacter* populations. The third term in Eq. [10] is the total rate of abiotic HNO_2 decomposition to NO

Table 2. Additional parameters used in simulations and sensitivity analysis.

Parameter		Value†			Units	Reference‡
		Case 1	Case 2	Case 3§		
$\mu_{max,1}$	max. growth rate, *Nitrosomonas*	0.031	0.031	0.036	h^{-1}	1
$B_{o,2}$	initial *Nitrobacter* population	1–10 (2) $\times 10^8$	2.0×10^8	1.0×10^8	cells kg^{-1} soil	2
$\mu_{max,2}$	max. growth rate, *Nitrobacter*	0.033–0.045 (0.036)	0.036	0.036	h^{-1}	1
$K_{I,2}$	inhibition factor for NO_2^- oxidation	#	$1–10^{-8.0}$ ($10^{-7.5}$)	$10^{-7.5}$	mole H^+ L^{-1}	¶
β_s	soil buffering capacity	30	20–40 (30)	20	mg H^+ kg^{-1} soil pH^{-1}	3
k_{PNO}	NO production rate coefficient	1.47×10^6	1.47×10^6	3.7×10^6	mg NO-N kg^{-1} N h^{-1}	4,5
k_{PN_2O}	N_2O production rate coefficient	1.1×10^4	1.1×10^4	3.2×10^4	mg N_2O-N kg^{-1} N h^{-1}	4,5
$K_{d,1}$	NH_4^+ phase partition coefficient	3.3×10^{-3}	3.3×10^{-3}	1.85×10^{-3}	$m^3\ H_2O\ kg^{-1}$ soil	6,7
$P_{b,5}$	background NO production rate	1.5×10^{-4}	1.5×10^{-4}	4×10^{-4}¶	mg N kg^{-1} soil h^{-1}	4
$P_{b,6}$	background N_2O production rate	0	0	1×10^{-2}	mg N kg^{-1} soil h^{-1}	¶
$k_{ox,5}$	NO oxidation rate coefficient	3.3×10^3	3.3×10^3	1.32×10^5¶	h^{-1}	4
$k_{red,6}$	N_2O reduction rate coefficient	0	0	8.0	h^{-1}	¶
–	depth of fertilizer incorporation	0–5	0–5	0–10	cm	¶,§

† Values in parentheses were used in examining model sensitivity to other parameters.
‡ 1 = Keen and Prosser, 1987; Prosser, 1989; 2 = Morrill and Dawson, 1967; Both et al., 1990; Degrange and Bardin, 1995; 3 = Curtin et al., 1996; Darrah et al., 1985; 4 = Venterea and Rolston, 2000a (Cases 1 and 2); 5 = Venterea and Rolston, 2000b (Case 3); 6 = Venterea and Rolston, unpublished data (Case 3); 7 = Wagenet et al., 1977 (Cases 1 and 2).
§ Initial conditions, bulk density, and water content were estimated from measured data (Venterea and Rolston, 2000b).
¶ Values set by authors.
# No inhibition of NO_2^- oxidation was assumed for Case 1.

and N_2O, where the liquid-phase HNO_2 concentration (g N m^{-3} H_2O) is calculated from the NO_2^- concentration, soil pH, and acid dissociation constant, as described in Venterea and Rolston (2000a). The parameters k_{PNO} and k_{PN_2O} are defined below. The present formulation also assumes that NO_2^- and H^+ in solution phase equilibrate to form HNO_2, and that soil pH reflects solution phase H^+ concentration. The rate of soil NO_3^- ($i = 3$) production will be controlled by the NOR as defined above. For H^+ ($i = 4$), it is assumed that production follows the stoichiometric generation of H^+ from autotrophic NH_4^+ oxidation, and also that HNO_2–mediated reactions consume H^+:

$$P_4 = \psi\left[\left(\frac{\partial C_{L,1}}{\partial t}\right)_{AOR} - \frac{1}{2}\theta k_{PNO}[HNO_2]_L\right] \quad [11]$$

where $\psi = 2$ g H^+ per 14 g N (Wang et al., 1998). The consideration of HNO_2 decomposition in consuming H^+ is based on experimental data showing that soil pH buffering is significantly increased during periods of high HNO_2–mediated NO production (Venterea and Rolston, 2000a) and also on Reaction [2] stoichiometry. For NO ($i = 5$), production is due primarily to abiotic HNO_2 decomposition, while consumption occurs due to liquid-phase oxidation and reduction and gas-phase oxidation:

$$P_5 = \theta\left(k_{PNO}[HNO_2]_L - \frac{C_{G,5}}{K_{H,5}}[k_{ox,5} + k_{red,5}(S_f)]\right) - \varepsilon k_{G,5}[O_2]C_{G,5}^2 + \rho P_{b,5} \quad [12]$$

where k_{PNO} is the rate coefficient for HNO_2–mediated NO production (Venterea and Rolston, 2000a), $k_{ox,5}$ describes first-order NO oxidation in the liquid phase (Venterea and Rolston, 2000a), $k_{red,5}$ describes first-order microbial NO reduction to N_2O as an increasing function of soil water saturation (S_f) (Venterea and Rolston, 2000b), and $k_{G,5}$ is a rate coefficient for NO oxidation by O_2 in the gas phase with second-order dependency on NO concentration (Atkinson et al., 1997) (O_2 concentration is assumed to be ambient). The additional production term ($P_{b,5}$) is based on data indicating that, in the absence of HNO_2, aerobically incubating soils exhibit a low but steady background NO production rate (i.e., <0.3 μg kg^{-1} h^{-1}) (Venterea and Rolston, 2000a). For N_2O ($i = 6$), liquid-phase production occurs through abiotic HNO_2 decomposition and microbial NO reduction:

$$P_6 = \theta\left(k_{PN_2O}[HNO_2]_L + k_{red,5}(S_f)\frac{C_{G,5}}{K_{H,5}}\right) - k_{red,6}\frac{C_{G,6}}{K_{H,6}} + \rho P_{b,6} \quad [13]$$

where k_{PN_2O} is the rate coefficient for HNO_2–mediated N_2O production (Venterea and Rolston, 2000a). The first-order reductive consumption coefficient ($k_{red,6}$) and background production term ($P_{b,6}$) are assumed to be mediated by denitrification processes and are therefore considered to be zero, except in comparisons with field data (Case 3, below).

Microbial Biomass Dynamics

Biomass kinetics are described by Monod growth with decay:

$$\frac{dB_i}{dt} = B_i\left[\frac{\mu_{max,i}C_{L,i}}{K_{s,i} + C_{L,i}} - d_i\right] \quad [14]$$

where B_i is the biomass density with $i = 1$ referring to *Nitrosomonas* and $i = 2$ to *Nitrobacter* biomass. It is assumed that cell maintenance energy is derived fully from endogenous decay, so decay coefficients (d_i) are calculated from published maintenance and yield coefficients for *Nitrosomonas* and *Nitrobacter* (Keen and Prosser, 1987; Herbert, 1959). The common observation that nitrification rates in soil tend to decrease with decreasing soil pH (e.g., Laanbroek and Woldendrop, 1995; Prosser, 1989) was modeled using a modified formulation of Quinlan's (1984) model describing pH effects on autotrophic NH_4^+ oxidation activity in liquid culture. Quinlan's (1984) complete three-parameter formulation was tested in preliminary simulations and found to significantly underestimate gross NH_4^+ oxidation rates measured concurrently with soil pH in incubating agricultural soils (Venterea and Rolston, 2000a). This discrepancy is probably related to the observation that autotrophic NH_4^+ oxidation proceeds in soil at much lower bulk pH than in well-mixed liquid systems, possibly due to microscale spatial variability in pH, surface effects, and/or acidophilic adaptations (Prosser, 1989; Hayatsu and Kosuge, 1993; Laanbroek and Woldendrop, 1995). The simplified one-parameter enzyme inhibition model

$$K_{s,i} = K_{s,i}^*\left(1 + \frac{10^{-pH}}{K_{I,i}}\right) \quad [15]$$

was found to more adequately describe decreases in measured gross NH_4^+ oxidation rates in soils, where $K_{I,i}$ is an inhibition constant and $K_{s,i}^*$ is the half-saturation concentration for growth in the absence of H^+ inhibition. An average value for $pK_{I,1}$ (where $pK_{I,i} = -\log_{10} K_{I,i}$) of 6.3 was obtained by comparison with data presented in Venterea and Rolston (2000a). This $pK_{I,1}$ value also adequately described NH_4^+ dynamics in a separate field study (data presented below) (Venterea and Rolston, 2000b). As a preliminary model, Eq. [15] was also used to describe H^+ inhibition of NO_2^- oxidation, and the inhibition parameter ($pK_{I,2}$) was evaluated over the range 6.5 to 8.0. While the above assumptions are certainly a simplification of the effects of pH on enzyme inhibition and substrate availability for autotrophic nitrifiers in soil, the formulation allows for at least a preliminary evaluation of how differential inhibition of the two classes of autotrophs can potentially affect NO_2^- accumulation and resulting gas emissions. Other potentially important inhibition effects not incorporated into the present model are discussed below.

Numerical Methods and Simulations

The partial differential equation (PDE) describing six chemical components (Eq. [3]) and the ordinary differential equation (ODE) describing two biomass populations (Eq. [14]) were solved simultaneously using numerical techniques based on Wu et al. (1990). Algorithms were validated by (i) material balance calculations computed at each time-step, (ii) comparison with exact solutions for single PDEs and for coupled systems of ODEs with linear reaction terms (Haberman, 1998), and (iii) convergence of solutions at decreasing time-step. Simulations presented were generated with maximum time-steps of 8×10^{-3} h and a 10^{-4} m spatial grid. Equation [3] was solved with no flux boundary conditions (BCs) for solutes ($i \leq 4$) at $z = 0$ (the soil surface) and $z = L$, where L is the depth of the soil profile. A value of 0.2 m for L was selected based on simulations that showed that use of greater L values had negligible effects on model output. For gases ($i \geq 5$), Eq. [3] was solved with no flux BCs at $z = L$, and constant concentration BCs with $C_i = C_{o,i}$ at $z = 0$, where $C_{o,i}$ is the atmospheric concentration of gaseous component i. Soil-to-atmosphere fluxes of NO and N_2O were calculated from Fick's law with the gradient estimated by the difference be-

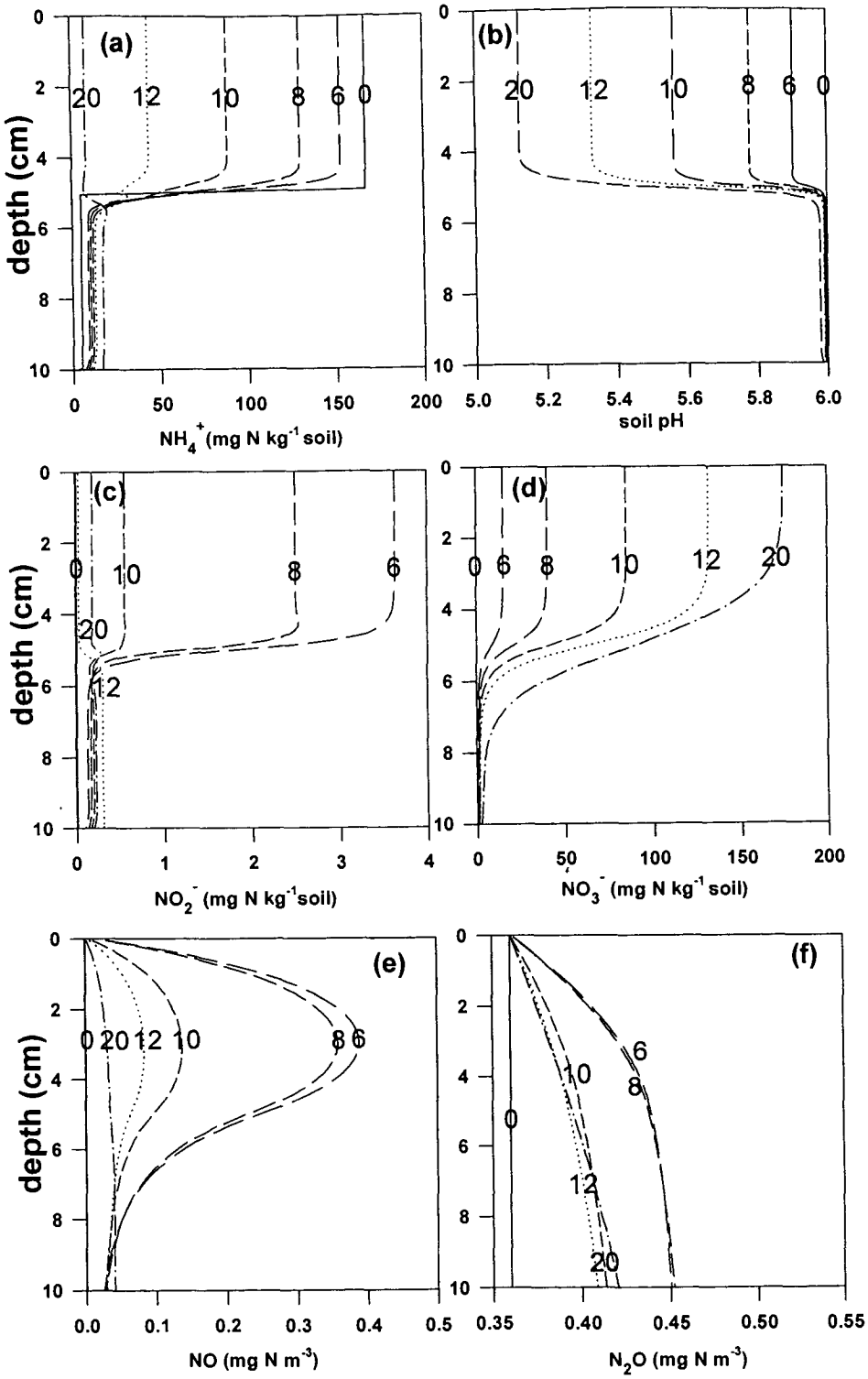

Fig. 2. Results of applying a mechanistic model of nitrite accumulation and N oxide gas emissions to a hypothetical uniform application of NH_4^+ fertilizer (100 kg N ha^{-1}) to the top 0 to 5 cm of soil of pH 6.0 (Case 1). Panels are concentration profiles after 0, 6, 8, 10, 12, and 20 d for (*a*) NH_4^+, (*b*) soil pH, (*c*) NO_2^-, (*d*) NO_3^-, (*e*) NO, and (*f*) N_2O.

tween $C_{o,i}$ and the concentration at the first subsurface node (z = 0.1 cm). The model was applied to two hypothetical fertilizer scenarios, Cases 1 and 2, to evaluate sensitivity to key input parameters (Tables 1 and 2). The initial conditions for Cases 1 and 2 consisted of uniform applications of NH_4^+ fertilizer within the top 0 to 5 cm of soil at 100 and 250 kg N ha^{-1}, and initial pH values of 6.0 and 8.0, respectively. A water content (θ) of 0.20 m^3 m^{-3} and bulk density (ρ) of 1200 kg m^{-3} were assumed. The effect of subsurface banding vs. surface incorporation was also examined for Cases 1 and 2.

Input parameters (Tables 1 and 2) for Cases 1 and 2 are taken directly from published data except for the H^+ inhibition factors ($K_{I,i}$), as discussed above. A range of growth rate ($\mu_{max,i}$) and half-saturation ($K_{s,i}^*$) values have been reported for *Nitro-*

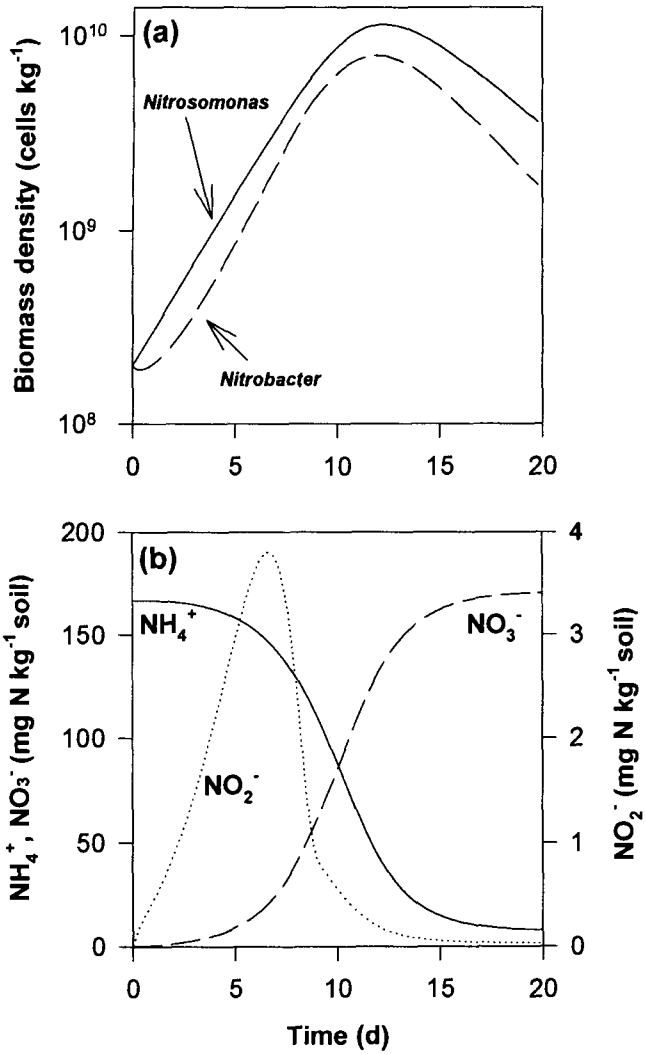

Fig. 3. Results of applying a mechanistic model of nitrite accumulation and N oxide gas emissions to a hypothetical uniform application of NH_4^+ fertilizer (100 kg N ha^{-1}) to the top 0 to 5 cm of soil of pH 6.0 (Case 1). Panels are (*a*) biomass population densities and (*b*) corresponding solute concentrations at center of incorporation depth (z = 2.5 cm).

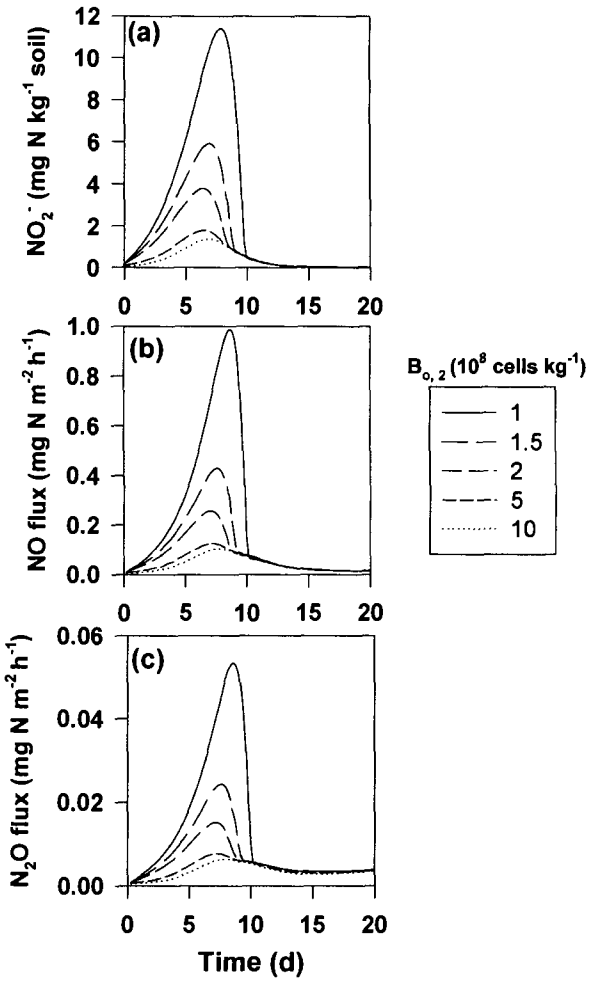

Fig. 4. Results of applying a mechanistic model of nitrite accumulation and N oxide gas emissions to a hypothetical uniform application of NH_4^+ fertilizer (100 kg N ha^{-1}) to the top 0 to 5 cm of soil of pH 6.0 (Case 1). Panels are (*a*) NO_2^- concentrations at center of incorporation depth and corresponding surface fluxes of (*b*) NO and (*c*) N_2O at varying values of initial *Nitrobacter* population density ($B_{o,2}$).

somonas and *Nitrobacter* (Prosser, 1989). For most of the simulations, the kinetic data of Keen and Prosser (1987) were used under the assumption that it is the most internally consistent data, since it is the only available data set based on similar methodologies for both populations and where corresponding yield and maintenance coefficients were also measured. Values reported by Morrill and Dawson (1967) for NH_4^+ oxidizer populations in agricultural soils are very similar to recent data (Bruns et al., 1999; Burns et al., 1995), and therefore 2×10^8 cells kg^{-1} soil was used as the initial *Nitrosomonas* population density ($B_{o,1}$) prior to fertilizer application in Cases 1 through 3. Some studies indicate that *Nitrobacter* populations tend to be higher and more highly variable than *Nitrosomonas* populations under neutral to acidic conditions, while in alkaline soils or soils receiving high inputs of alkaline-producing fertilizers, *Nitrobacter* populations tend to be suppressed (Morrill and Dawson, 1967; Both et al., 1990; Degrange and Bardin, 1995; Burns et al., 1995). These trends suggest that NH_3 toxicity, which is expected to be more important under alkaline conditions, may have effects on the initial viable *Nitrobacter* population density. Therefore, a range of values was examined for initial *Nitrobacter* population density ($B_{o,2}$ = 1–10 $\times$ 10^8 cells kg^{-1} soil) in Case 2, where the initial soil pH was assumed to be 8.0.

For Case 3, data from a previously published field study (Venterea and Rolston, 2000b) were compared with model simulations. In this study, anhydrous NH_3 was applied to a tomato field comprised of a moderately acidic (pH = 5.3) loam (11% clay) over 0 to 20 cm depth at 120 kg N ha^{-1} in 15-cm-wide bands spaced 25 to 35 cm from each row on both sides. Parameters (Table 2) were selected from within the range of values examined in the sensitivity analyses, except for values of $k_{ox,5}$, $P_{b,5}$, $k_{red,6}$, and $P_{b,6}$, which were selected by trial and error for best fit to the data (discussed below).

RESULTS AND DISCUSSION

Case 1 (100 kg N ha^{-1}, initial pH = 6.0)

Concentration profiles for N solutes, gases, and soil pH shown in Fig. 2 are indicative of nitrification, which is nearly complete by 20 d. A transient accumulation of NO_2^- is predicted (Fig. 2c). The decrease in soil pH

Table 3. Effect of inhibition factor ($K_{I,2}$), buffering capacity (β_s) and subsurface fertilizer placement on Case 2 simulation results.

			Peak flux		Total emissions†		Peak concentration
$K_{I,2}$	β_s	Depth¶	NO	N_2O	NO	N_2O	NO_2^-
mol H^+ L^{-1}	mg H^+ kg^{-1} pH^{-1}	cm	— mg N m^{-2} h^{-1}‡ —		— kg N ha^{-1}‡ —		mg N kg^{-1}
§	30	0–5	2.3	0.12	0.61	0.033	60
$10^{-6.5}$	30	0–5	2.7	0.13	0.71	0.037	64
$10^{-7.5}$	30	0–5	5.5	0.27	1.6	0.084	100
$10^{-8.0}$	30	0–5	10.0	0.50	4.4	0.22	160
$10^{-7.5}$	20	0–5	23.0	1.20	20	1.0	94
$10^{-7.5}$	25	0–5	11.0	0.55	4.1	0.22	98
$10^{-7.5}$	30	0–5	5.5	0.27	1.6	0.084	100
$10^{-7.5}$	40	0–5	1.8	0.09	0.55	0.029	100
$10^{-7.5}$	30	0–5	5.5	0.27	1.6	0.084	100
$10^{-7.5}$	30	1–6	2.0	0.27	0.64	0.086	100
$10^{-7.5}$	30	2.5–7.5	0.72	0.28	0.24	0.090	100
$10^{-7.5}$	30	5–10	0.13	0.29	0.056	0.092	100

† Total integrated emissions over 20 d.
‡ 1 kg N ha^{-1} = 100 mg N m^{-2}.
§ No inhibition of NO_2^- oxidation was assumed in this simulation.
¶ Initial vertical distribution of fertilizer at rate of 250 kg N ha^{-1}.

(Fig. 2b) results in HNO_2 formation and abiotic NO production (Fig. 2e). Decomposition of HNO_2 together with NO reduction results in N_2O production (Fig. 2f). Predicted biomass and N solute dynamics at the center of the incorporation depth (z = 2.5 cm) display a pattern of *Nitrobacter* lag concurrent with more rapid *Nitrosomonas* growth (Fig. 3a) and transient NO_2^- accumulation (Fig. 3b). These results are very similar to patterns observed in 56 of 100 soils (all with pH <7.3) examined in soil percolation studies by Morrill and Dawson (1967). Similar temporal patterns and peak NO_2^- concentrations (0.2 to 10 mg N kg^{-1} soil) have been observed in several other nitrification studies under neutral to acidic conditions following N applications (Chapman and Leibeg, 1952; Jones and Hedlin, 1970; Paul and Domsch, 1972).

In the above simulation (Fig. 3), NO_2^- accumulates even though initial *Nitrobacter* and *Nitrosomonas* populations are equivalent and the kinetic parameters ($\mu_{max,i}$, $K^*_{s,i}$) favor more rapid growth of *Nitrobacter* compared with *Nitrosomonas* (Tables 1 and 2). At higher initial *Nitrobacter* population densities (up to 10^9 cells kg^{-1}), NO_2^- still accumulates (Fig. 4a). Varying the maximum *Nitrobacter* specific growth rate ($\mu_{max,2}$) over the range 0.050 to 0.033 h^{-1} (Prosser, 1989) produced peak NO_2^- concentrations of 0.3 to 10 mg N kg^{-1}, respectively, with the same temporal patterns. Varying the decay (d_i) or yield coefficients (Y_i) over a range of literature values, or removal of the decay term from either or both of the biomass expressions had a similar range of effects (not shown).

Kinetic Basis for Nitrite Accumulation

The above results suggest that some degree of transient NO_2 accumulation following NH_4^+ addition is a consequence of the nature of nitrification itself, that is, as a two-step sequential process carried out by distinct microbial populations. High NH_4^+ levels stimulate *Nitrosomonas* growth and NO_2^- production, while *Nitrobacter* growth rates are initially limited by lower substrate (NO_2^-) levels. Eventually, *Nitrobacter* growth and activity increase to match the rate of NO_2^- supplied by *Nitrosomonas* activity (Fig. 3). The simulation results demonstrate how reductions in initial *Nitrobacter* population densities ($B_{o,2}$) (Fig. 4a) and/or growth rates ($\mu_{max,2}$), which may occur in response to NH_3 or other chemical toxicity effects, can enhance the extent of NO_2^- accumulation. The results also suggest that diversity of autotrophic populations with respect to growth and substrate utilization kinetics may be responsible for observed variabilities in NO_2^- accumulation across a range of soil environments.

Transient Nitrogen Oxide Emissions

The peak NO fluxes (0.10–1.0 mg N m^{-2} h^{-1}) and the temporal patterns predicted by the model (Fig. 4b) are within the range observed in several field studies following the addition of NH_4^+ salts under acidic to slightly alkaline conditions (Johansson and Galbally, 1984; Slemr and Seiler, 1984; Shepherd et al., 1991; Slemr and Seiler, 1991; Hutchinson and Brams, 1992; Thornton and Valente, 1996). The magnitude of the predicted N_2O pulses (<0.06 mg N m^{-2} h^{-1}) (Fig. 4c) is generally less than that observed following similar fertilizer applications. This is probably due to N_2O derived from biological reductions of NO_3^- and/or NO_2^-, which are not accounted for by the present model.

Case 2 (250 kg N ha^{-1}, initial pH = 8.0)

For Case 2, the predicted peak NO_2^- concentrations and gas fluxes, assuming no pH effects on *Nitrobacter* activity, are significantly higher than in Case 1 (Table 3). Additional simulations indicated that the more favorable (i.e., slightly alkaline) initial pH resulted in more rapid NH_4^+ oxidation rates given the same initial NH_4^+ concentrations, thereby leading to higher peak NO_2^- concentrations. For $pK_{I,2}$ values ≥6.5, significant increases in peak NO_2^- levels, peakfl uxes, and total gas emissions are predicted (Table 3). The predicted maximum soil NO_2^- concentrations (60–160 mg NO_2^-–N kg^{-1}) are similar to those observed following the application of urea, anhydrous ammonia, or other N fertilizers under moderately alkaline conditions (Martin et al., 1942; Chapman and Leibeg, 1952; Chalk et al., 1975; Jones and Hedlin, 1970). The role of NH_3 toxicity under these

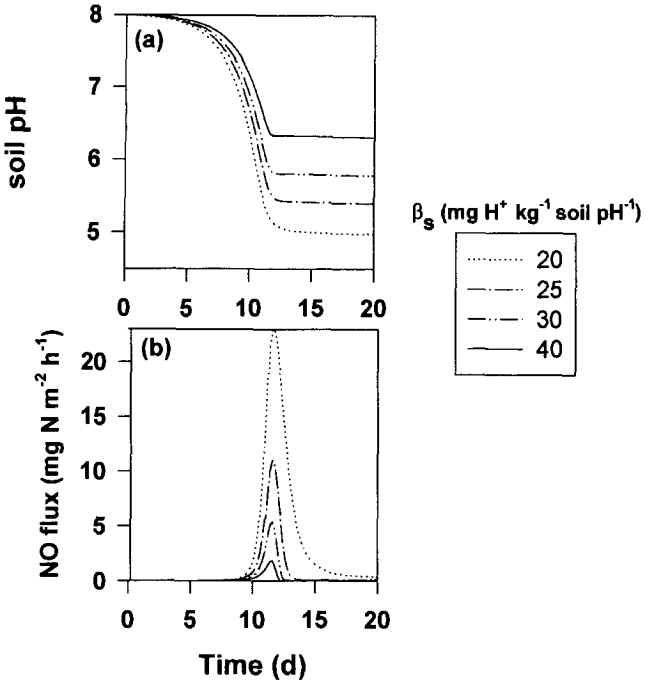

Fig. 5. Results of applying a mechanistic model of nitrite accumulation and N oxide gas emissions to a hypothetical uniform application of NH_4^+ fertilizer (250 kg N ha^{-1}) to the top 0 to 5 cm of soil of pH 8.0 (Case 2). Panels are (*a*) soil pH at center of incorporation depth and (*b*) surface NO flux at varying values of buffering capacity (β_s).

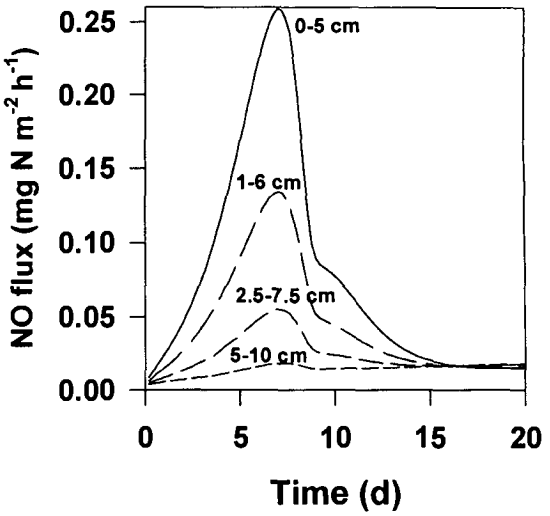

Fig. 6. Results of applying a mechanistic model of nitrite accumulation and N oxide gas emissions to a hypothetical uniform application of NH_4^+ fertilizer (100 kg N ha^{-1}) to soil of pH 6.0 (Case 1). Shown are predicted NO fluxes for fertilizer applied in 5-cm layers at varying soil depth (Case 2 results are given in Table 3).

conditions is more likely to be important, which is partly accounted for in the present model by limiting the initial viable *Nitrobacter* density to 2×10^8 cells kg^{-1}. The predicted peak NO fluxes (2–10 mg N m^{-2} h^{-1}) (Table 3) are also within the range of maximum fluxes observed under similar fertilizer conditions (Slemr and Seiler, 1984; Thornton et al., 1996; Matson et al., 1998).

Buffering Capacity Effects

The dynamics of soil pH as influenced by buffering capacity (β_s) had significant effects, with predicted peak gas fluxes and total emissions increasing by >90% as β_s is decreased from 40 to 20 mg H$^+$ kg^{-1} soil pH^{-1} (Fig. 5, Table 3). Thus, soils with coarser texture and lower organic matter content, which are generally less buffered against pH changes (Curtin et al., 1996), would be expected to emit much more N oxide gas given similar fertilizer inputs and N dynamics.

Surface vs. Subsurface Fertilizer Incorporation

Predicted NO fluxes were increasingly attenuated with increasing depth of fertilizer incorporation for Case 1 (Fig. 6) and Case 2 (Table 3) due to microbial and chemical transformation of NO as it diffuses to the surface. This general effect has been observed in field studies (Matson et al., 1996). The present model predicts that placement over a depth of 5 to 10 cm would result in reductions in total NO emissions of >76% and >98% compared with surface applications (0–5 cm) for Cases 1 and 2, respectively. The model does not consider potential increases in denitrification-derived N_2O production that might occur due to the same practice.

Case 3: Comparison with Field Data

The general temporal dynamics of N solutes, soil pH, and NO and N_2O fluxes are described fairly well using input parameters in Table 2 (Fig. 7). Part of the discrepancy between simulated values and observed data is probably due to the assumption of spatially uniform initial conditions, especially since banded anhydrous NH_3 applications generally result in highly heterogenous NH_4^+ distributions (Moraghan, 1980). The need for increased values of $P_{b,5}$ and $P_{b,6}$ in order to approximate the observed flux data is probably due to source processes, including denitrification, occurring at depths >20 cm. The need for increased values of the transformation parameters $k_{ox,5}$ and $k_{red,6}$ may be due to more rapid and/or unaccounted for sinks under field conditions. For example, as discussed by Venterea and Rolston (2000b), horizontal subsurface gaseous diffusion resulting from lateral gradients in HNO_2 concentrations may have resulted in attenuated gas fluxes directly above the fertilizer band at this site. Expanding the present model to include two-dimensional transport would require a significant increase in complexity, but may be required in order to adequately predict fluxes that are driven by geometrically nonuniform processes. Additional uncertainty in modeling Case 3 arises from the unknown initial conditions and N dynamics over the 10- to 20-cm depth, since intensive sampling in the previous study was limited to the 0- to 10-cm depth. In these simulations, the 10- to 20-cm depth was assumed to provide a background source (described by $P_{b,5}$ and $P_{b,6}$) and also a sink for NO and N_2O. The predicted low recovery of NO_3^- compared with the amount of added NH_4^+ (Fig. 7a,b) is due to the production, transformation, and escape of N oxide gases considered by the

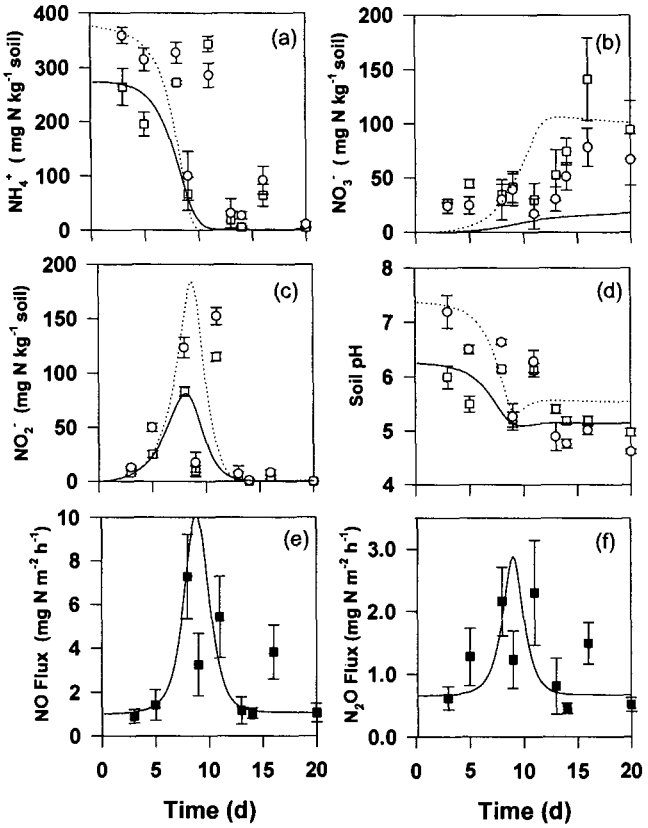

Fig. 7. Results of applying a mechanistic model of nitrite accumulation and N oxide gas emissions to an actual application of anhydrous NH_4^+ fertilizer to an acidic loam (Case 3, from Venterea and Rolston, 2000b). Panels are data (symbols) and model predictions (lines) of (*a*) NH_4^+, (*b*) NO_3^-, (*c*) NO_2^-, and (*d*) soil pH averaged over 0 to 5 cm (open square, solid line) and 5 to 10 cm (open circle, dashed line) and (*e*) NO and (*f*) N_2O fluxes.

model. While the predicted NO and N_2O emissions accounted for only 3.3 and 1.3%, respectively, of the NH_4^+ initially present in the upper 10 cm, the high liquid-phase NO consumption rate ($k_{ox,5}$ = 1.3 × 10^5 h^{-1}) resulted in most of the remaining discrepancy. In reality, a large fraction of the NO oxidized may well be converted to NO_3^- (Conrad, 1995b). This conversion was not accounted for by the model (i.e., the oxidized NO was not allocated to a specific N pool).

While the predicted N solute dynamics are consistent with data in the above-referenced studies, other data from liquid culture and soil studies suggest that enzyme inhibition kinetics of autotrophic nitrifiers are likely to be more complex than assumed here. The inhibition of NH_4^+ oxidation due to NH_3 toxicity and/or inhibition of NH_4^+ and NO_2^- oxidation due to accumulations of NO_2^-, HNO_2, or NO_3^- are not considered in the present model. Preliminary simulations indicate that these effects may be responsible for the more prolonged duration of NO_2^- accumulation (up to several months) observed in some field studies (Chalk et al., 1975; Chapman and Leibeg, 1952). Quantitative models have been developed to describe some of these effects in liquid systems (Boon and Laudelout, 1962; Hunik et al., 1993). However, the applicability of these models to soil systems has not been examined, and therefore it would be premature to include them in the present model.

CONCLUSIONS

The model of N transformation and transport presented here describes how interactions between biological, chemical, and physical processes can regulate N oxide gas emissions under conditions favoring nitrification in soil. An advantage of this modeling approach is the capability to examine quantitative effects of multiple complex interactions under transient conditions that cannot be considered using more simple approaches. The results have direct implications with respect to fertilizer management practices. For example, the results indicate that (i) soils receiving similar fertilizer treatments, but differing in their ability to buffer nitrification-induced acidity, may produce dramatically different N oxide emissions; (ii) subsurface fertilizer incorporation can significantly reduce, and in some cases nearly eliminate, net NO emissions; and (iii) the differential responses of *Nitrosomonas* and *Nitrobacter* populations to chemical toxicities associated with the form and/or rate of fertilizer application may significantly affect the extent of NO_2^- accumulation and corresponding gas emissions. Further investigations are required in order to better model the behavior of autotrophic nitrifying populations in response to a range of dynamic chemical conditions. Few field studies exist, and more are required, involving simultaneous measurements of soil pH, N substrate concentrations, and gas fluxes, so that detailed mechanistic models can be compared against actual data. Models of this type will also benefit from more basic investigations of the functional diversity of autotrophic nitrifying microbes under differing ecological conditions. Consideration of additional mechanisms of NO and N_2O production not included in the present model, including microbial reduction mediated by denitrifying (and possibly nitrifying) soil bacteria, is also required in order to more fully describe the underlying mechanisms of N oxide gas production under field conditions.

ACKNOWLEDGMENTS

The authors gratefully acknowledge K. Scow, W. Horwath, and J. Hopmans for their reviews of an earlier version of the manuscript, and three anonymous reviewers for their helpful suggestions. This work was supported in part by the Kearney Foundation of Soil Science and in part by the USEPA (R819658 & 825433) Center for Ecological Health Research at UC Davis, although it may not necessarily reflect the views of the USEPA, and no official endorsement should be inferred.

REFERENCES

Ardakani, M., J. Rehbock, and A. McLaren. 1974. Oxidation of ammonium to nitrate in a soil column. Soil Sci. Soc. Am. Proc. 38:96–99.

Atkinson, R., D. Baulch, R. Cox, J.R. Hampson, J. Kerr, M. Rossi, and J. Troe. 1997. Evaluated kinetic and photochemical data for atmospheric chemistry: Supplement VI. IUPAC subcommittee on gas kinetic data evaluation for atmospheric chemistry. J. Phys. Chem. Ref. Data 26:1329–1499.

Bezdicek, D., J. MacGregor, and W. Martin. 1971. The influence of soil-fertilizer geometry on nitrification and nitrite accumulation. Soil Sci. Soc. Am. Proc. 35:997–1002.

Bird, R., W. Stewart, and E. Lightfoot. 1960. Transport phenomena. John Wiley & Sons, New York.

Boon, B., and H. Laudelout. 1962. Kinetics of nitrite oxidation by *Nitrobacter winogradskyi*. Biochem. J. 85:440–447.

Both, G., S. Gerards, and H. Laanbroek. 1990. Enumeration of nitrite-oxidizing bacteria in grassland soils using a most probable number technique: Effect of nitrite concentration and sampling procedure. FEMS Microbiol. Ecol. 74:277–285.

Bruns, M., J. Stephen, G. Kowalchuk, J. Prosser, and E. Paul. 1999. Comparative diversity of ammonia oxidizer 16S rRNA gene sequences in never-tilled, tilled, and successional soils. Appl. Environ. Microbiol. 65:2994–3000.

Burns, L., R. Stevens, R. Smith, and J. Cooper. 1995. The occurrence and possible sources of nitrite in a grazed, fertilized, grassland soil. Soil Biol. Biochem. 27:47–59.

Chalk, P., D. Keeney, and L. Walsh. 1975. Crop recovery and nitrification of fall and spring applied anhydrous ammonia. Agron. J. 67:33–41.

Chapman, H., and G. Leibeg, Jr. 1952. Field and laboratory studies of nitrite accumulation in soils. Soil Sci. Soc. Am. Proc. 16:276–282.

Conrad, R. 1995a. Soil microbial processes involved in production and consumption of atmospheric trace gases. p. 207–250. *In* J. Jones (ed.) Advances in microbial ecology. Plenum Press, New York.

Conrad, R. 1995b. Metabolism of nitric oxide in soil and soil microorganisms and regulation of flux into the atmosphere. p. 167–201. *In* J.C. Murrell and D.P. Kelly (ed.) Microbiology of atmospheric trace gases/sources, sinks and global processes. NATO ASI Series I, Global Environment Change. Vol. 39. Springer, New York.

Crutzen, P. 1981. Atmospheric chemical processes of the oxides of nitrogen, including nitrous oxide. p. 17–44. *In* C. Delwiche (ed.) Denitrification, nitrification and atmospheric N_2O. John Wiley & Sons, Chichester, UK.

Curtin, D., C. Campbell, and A. Jalil. 1998. Effects of acidity on mineralization: pH-dependence of organic matter mineralization in weakly acidic soils. Soil Biol. Biochem. 30:57–64.

Curtin, D., C. Campbell, and D. Messer. 1996. Prediction of titratable acidity and soil sensitivity to pH change. J. Environ. Qual. 25: 1280–1284.

Darrah, P.R., R.E. White, and P.H. Nye. 1985. Simultaneous nitrification and diffusion in soil. I. The effects of the addition of a low level of ammonium chloride. J. Soil Sci. 36:281–292.

Davidson, E., and W. Kingerlee. 1997. A global inventory of nitric oxide emissions from soils. Nutr. Cycl. Agroecosyst. 48:37–50.

Degrange, V., and R. Bardin. 1995. Detection and counting of *Nitrobacter* populations in soil by PCR. Appl. Environ. Microbiol. 61:2093–2098.

Firestone, M., and E. Davidson. 1989. Microbiological basis of NO and N_2O production and consumption in soil. p. 7–21. *In* M. Andreae and D. Schimel (ed.) Exchange of trace gases between terrestrial ecosystems and the atmosphere. John Wiley & Sons, Chichester, UK.

Grant, R. 1995. Mathematical modelling of nitrous oxide evolution during nitrification. Soil Biol. Biochem. 27:1117–1125.

Haberman, R. 1998. Elementary applied partial differential equations: With Fourier series and boundary value problems. Prentice Hall, New Jersey.

Hayatsu, M., and N. Kosuge. 1993. Autotrophic nitrification in acid tea soils. Soil Sci. Plant Nutr. 39:209–217.

Herbert, D. 1959. Some principles of continuous culture. p. 381–396. *In* G. Tunevall (ed.) Recent progress in microbiol. Almquist and Wicksell, Stockholm.

Hunik, J., C. Bos, M. van den Hoogen, C. De Gooijer, and J. Tramper. 1994. Co-immobilized *Nitrosomonas europaea* and *Nitrobacter agilis* cells: Validation of a dynamic model for simultaneous substrate conversion and growth in *k*-carrageenan gel beads. Biotech. Bioeng. 43:1153–1163.

Hunik, J., H. Meijer, and J. Tramper. 1993. Kinetics of *Nitrobacter agilis* at extreme substrate, product and salt concentrations. Appl. Microbiol. Biotechnol. 40:442–448.

Hutchinson, G., and E. Brams. 1992. NO versus N_2O emissions from an NH_4–amended Bermuda grass pasture. J. Geophys. Res. 97: 9889–9896.

Johansson, C., and I. Galbally. 1984. Production of nitric oxide in loam under aerobic and anaerobic conditions. Appl. Environ. Microbiol. 47:1284–1289.

Jones, R., and R. Hedlin. 1970. Ammonium, nitrite and nitrate accumulation in three Manitoba soils as influenced by added ammonium sulfate and urea. Can. J. Soil Sci. 50:331–338.

Keen, G., and J. Prosser. 1987. Steady state and transient growth of autotrophic nitrifying bacteria. Arch. Microbiol. 147:73–79.

Kelso, B., R. Smith, and R. Laughlin. 1999. Effects of carbon substrates on nitrite accumulation in freshwater sediments. Appl. Environ. Microbiol. 65:61–66.

Kemper, W. 1986. Solute diffusivity. p. 1007–1024. *In* A. Klute (ed.) Methods of soil analysis. Part 1. Physical and mineralogical methods. Agron. Monogr. 9. ASA, Madison, WI.

Laanbroek, H., and J. Woldendrop. 1995. Activity of chemolithotrophic nitrifying bacteria under stress in natural soils. p. 275–304. *In* J. Jones (ed.) Advances in microbial ecology. Plenum Press, New York.

Li, C., S. Frolking, and T.A. Frolking. 1992. A model of nitrous oxide evolution from soil driven by rainfall events: 1. Model structure and sensitivity. J. Geophys. Res. 97(D9):9759–9776.

Martin, W., T. Buehrer, and A. Caster. 1942. Threshold pH value for the nitrification of ammonia in desert soils. Soil Sci. Soc. Am. Proc. 7:223–228.

Matson, P. 1997. NO_x emission from soils and its consequences for the atmosphere and biosphere: Critical gaps and research directions for the future. Nutr. Cycl. Agroecosyst. 48:1–6.

Matson, P., C. Billow, and S. Hall. 1996. Fertilization practices and soil variations control nitrogen oxide emissions from tropical sugar cane. J. Geophys. Res. 101(D13):18 533–18 545.

Matson, P., R. Naylor, and I. Ortiz-Monasterio. 1998. Integration of environmental, agronomic, and economic aspects of fertilizer management. Science 280:112–115.

Moldrup, P., T. Olesen, D. Rolston, and T. Yamaguchi. 1997. Modeling diffusion and reaction in soils: VII. Predicting gas and ion diffusivity in undisturbed and sieved soils. Soil Sci. 162:632–640.

Moraghan, J. 1980. Precautions on the use of anhydrous ammonia applicators in research plots. Agron. J. 72:157–160.

Morrill, L., and J. Dawson. 1967. Patterns observed for the oxidation of ammonium to nitrate by soil organisms. Soil Sci. Soc. Am. Proc. 31:757–760.

Mosier, A., J. Duxbury, J. Freney, O. Heinemeyer, and K. Minami. 1996. Nitrous oxide emissions from agricultural fields: Assessment, measurement and mitigation. Plant Soil 181:95–108.

Nelson, D. 1982. Gaseous losses of nitrogen other than through denitrification. p. 327–364. *In* F. Stevenson (ed.) Nitrogen in agricultural soils. ASA, CSSA, and SSSA, Madison, WI.

Nye, P. 1972. The measurement and mechanism of ion diffusion in soils. VII. A theory for the propogation of changes of pH in soils. J. Soil Sci. 23:82–92.

Paul, W., and K. Domsch. 1972. Ein mathemathisches modell fur nitrifikationsprozeb im boden. Arch. Microbiol. 87:77–92.

Prosser, J. 1989. Autotrophic nitrification in bacteria. Adv. Microb. Physiol. 30:125–181.

Quinlan, A. 1984. Prediction of the optimum pH for ammonia-N oxidation by *Nitrosomonas europaea* in well-aerated natural and domestic-waste waters. Water Resour. 18:561–566.

Shepherd, M., S. Barzetti, and D. Hastie. 1991. The production of atmospheric NO_x and N_2O from a fertilized agricultural soil. Atmos. Environ. 25A:1961–1969.

Slemr, F., and W. Seiler. 1984. Field measurements of NO and NO_2 emissions from fertilized and unfertilized soils. J. Atmos. Chem. 2:1–24.

Slemr, F., and W. Seiler. 1991. Field study of environmental variables controlling the NO emissions from soil and the NO compensation point. J. Geophys. Res. 96:13 017–13 031.

Stevenson, F. 1994. Humus chemistry: Genesis, composition, reactions. John Wiley & Sons, New York.

Suzuki, I., U. Dular, and S. Kwok. 1974. Ammonia or ammonium ion as substrate for oxidation by *Nitrosomonas europaea* cells and extracts. J. Bacteriol. 120:556–558.

Thornton, F., B. Bock, and D. Tyler. 1996. Soil emissions of nitric oxide and nitrous oxide from injected anhydrous ammonium and urea. J. Environ. Qual. 25:1378–1384.

Thornton, F.C., and R.J. Valente. 1996. Soil emissions of nitric oxide and nitrous oxide from no-till corn. Soil Sci. Soc. Am. J. 60: 1127–1133.

Van Cleemput, O., W. Patrick, and R. McIlhenny. 1976. Nitrite decomposition in flooded soil under different pH and redox potential conditions. Soil Sci. Soc. Am. J. 40:55–60.

Van Cleemput, O., and A. Samater. 1996. Nitrite in soils: Accumulation and role in the formation of gaseous N compounds. Fert. Res. 45:81–89.

Venterea, R., and D. Rolston. 2000a. Mechanisms and kinetics of nitric and nitrous oxide production during nitrification in agricultural soil. Global Change Biol. 6:303–316.

Venterea, R., and D. Rolston. 2000b. Nitric and nitrous oxide emissions following fertilizer application to agricultural soil: Biotic and abiotic mechanisms and kinetics. J. Geophys. Res. 105 (D12):15 117–15 129.

Wagenet, R., J. Biggar, and D. Nielsen. 1977. Tracing the transformation of urea fertilizer during leaching. Soil Sci. Soc. Am. J. 41: 896–902.

Wang, F., J. Bear, and A. Shaviv. 1998. Modelling simultaneous release, diffusion and nitrification of ammonium in the soil surrounding a granule or nest containing ammonium fertilizer. Eur. J. Soil Sci. 49:351–364.

Wilhelm, E., R. Battino, and R.J. Wilcock. 1977. Low-pressure solubility of gases in water. Chem. Rev. 77:219–262.

Williams, E., A. Guenther, and F. Fehsenfeld. 1992. An inventory of nitric oxide emissions from soils in the United States. J. Geophys. Res. 97(D7):7511–7519.

Wu, J.C., L.T. Fan, and L.E. Erickson. 1990. Three-point backward finite-difference method for solving a system of mixed hyperbolic-parabolic partial differential equations. Comp. Chem. Eng. 14: 679–685.